

Closing of the pseudogap in $\text{La}_{2-z-x}\text{Nd}_z\text{Sr}_x\text{CuO}_4$ ($z = 0, 0.4$)

Manfred Bucher

Physics Department, California State University, Fresno,

Fresno, California 93740-8031

(Dated: October 10, 2021)

Abstract

Doping of La_2CuO_4 and $\text{La}_{1.6}\text{Nd}_{0.4}\text{CuO}_4$ with Sr gives rise to holes that locate pairwise at lattice-site O atoms. Such O atoms reside as lattice defects in the CuO_2 planes if the doping level x is below a watershed value, $x < \hat{x}$, but also in the bracketing LaO layers if $x > \hat{x}$. The O atoms form a 2D charge order of incommensurability $q_{CO}^{\text{CuO}_2}(x)$ and $q_{CO}^{\text{LaO}}(x)$. At the doping x^* (quantum critical point) that causes the closing of the pseudogap at $T = 0$, $q_{CO}^{\text{CuO}_2}(x^*) = 2q_{CO}^{\text{LaO}}(x^*)$ holds.

I. CHARGE ORDER IN $\text{La}_{2-x}\text{Sr}_x\text{CuO}_4$

When La_2CuO_4 is doped with strontium, substitution of $\text{La} \rightarrow \text{La}^{3+} + 3e^-$ by $\text{Sr} \rightarrow \text{Sr}^{2+} + 2e^-$ causes a lack of electrons, or equivalently, a creation of holes. Coulomb repulsion spreads the holes, which then attach pairwise to oxygen in the CuO_2 planes, $\text{O}^{2-} + 2e^+ \rightarrow \text{O}$. There the O atoms form a charge order (CO) by a 2D superlattice. The reciprocal of the superlattice spacing, $A_0(x) \simeq B_0(x)$, is called the incommensurability,¹

$$\frac{1}{A_0(x)} \equiv q_{CO}^{\text{CuO}_2}(x) = \frac{\Omega^\pm}{2} \sqrt{x - \tilde{p}}, \quad x < \hat{x}. \quad (1)$$

In the medium doping range, $0.10 \lesssim x \lesssim 0.15$, the charge order manifests as unidirectional stripes, at higher doping as nematicity. The formula, in reciprocal lattice units (r.l.u.), is valid for doping up to a “watershed” concentration \hat{x} , which depends on the species of doping. The stripe-orientation factor is $\Omega^+ = \sqrt{2}$ for $x > x_6 = 2/6^2 \simeq 0.056$ when stripes are parallel to the a or b axis, but $\Omega^- = 1$ for $x < x_6$ when stripes are diagonal. The offset value \tilde{p} under the radical is the hole concentration necessary to keep three-dimensional antiferromagnetism (3D-AFM) suppressed. Their skirmisher task keeps those “suppressor holes” from participating in charge order.

Also because of Coulomb repulsion, the doped-hole concentration saturates in the CuO_2 planes at \hat{x} , causing the square-root curve from Eq.(1) to level off, with increased doping, to a constant plateau (depending on dopant and co-dopant species),¹

$$q_{CO}^{\text{CuO}_2}(x) = \frac{\sqrt{2}}{2} \sqrt{\hat{x} - \tilde{p}}, \quad x \geq \hat{x}, \quad (2)$$

(see Fig. 1). Additional doped holes then overflow to the LaO layers that sandwich the CuO_2 planes, where they also reside pairwise in (apical) O atoms. Again, Coulomb repulsion spreads the double holes to a planar superlattice of lattice-defect O atoms in *each* LaO layer, with attending charge order of incommensurability¹

$$q_{CO}^{\text{LaO}}(x) = \frac{\sqrt{2}}{2} \sqrt{\frac{x - \hat{x}}{2}}, \quad x \geq \hat{x}. \quad (3)$$

The denominator 2 under the radical is due to the two LaO layers per unit cell.

The Sr doping that causes the closing of the pseudogap at $T = 0$ is denoted as x^* . It is widely regarded a quantum critical point. Inserting the observed data of \hat{x} , \tilde{p} , and x^* of $\text{La}_{2-x}\text{Sr}_x\text{CuO}_4$ from Table I into Eqs. (2, 3) gives incommensurabilities

$$2q_{CO}^{\text{LaO}}(x^*) = q_{CO}^{\text{CuO}_2}(\hat{x}) = q_{CO}^{\text{CuO}_2}(x^*). \quad (4)$$

For the sake of graphic visualization we combine the defect-charge order of the upper LaO layer (\overline{LaO}) and lower LaO layer (\underline{LaO}), staggered by half a superlattice spacing, $\frac{1}{2}A_0^{LaO} = \frac{1}{2}/q_{CO}^{LaO}$ (see Fig. 2), such that *together* they form a charge order of incommensurability

$$q_{CO}^{\overline{LaO}+\underline{LaO}}(x) = 2q_{CO}^{LaO}(x) = \sqrt{x - \hat{x}}. \quad (5)$$

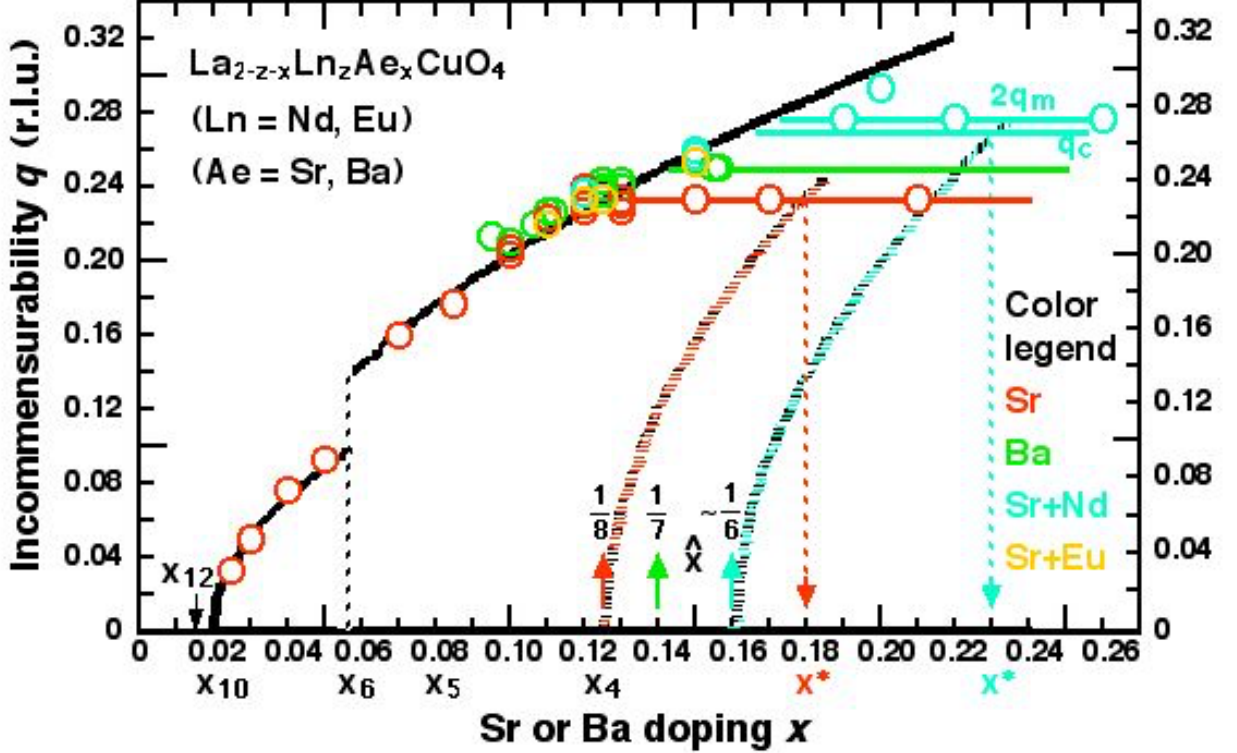


FIG. 1. Incommensurability of O superlattice charge order, $q = q_c$, and O superlattice magnetization, $q = 2q_m$, in the CuO_2 planes (solid curves and horizontal lines) and in the LaO layers (hatched curves) of $La_{2-z-x}Ln_zAe_xCuO_4$ ($Ln = Nd, Eu; z = 0, 0.4, 0.2$) due to doping with $Ae = Sr$ or Ba . Commensurate doping concentrations are denoted by $x_n \equiv 2/n^2$. Circles show data from X-ray diffraction and scattering or neutron scattering. For $La_{1.6}Nd_{0.4}Sr_xCuO_4$ the $2q_m$ data are experimental, the horizontal q_c line is inferred (see text). The broken black curve is a graph of Eq. (1), calculated with a constant offset value, $\tilde{p} = x_{10} = 0.02$. Its discontinuity at $x_6 \simeq 0.056$ is caused by a change of stripe orientation, relative to the planar crystal axes, from diagonal for $x < x_6$ to parallel for $x > x_6$. The solid (colored) horizontal lines are graphs of Eq. (2) and the hatched colored curves are graphs of $2q_c^{LaO}(x)$, Eqs. (3, 5). The condition for closing of the pseudogap, Eq. (4), is illustrated by the dashed down arrows.

TABLE I: Watershed concentration \hat{x} of doped Sr where the square-root curve of charge-order incommensurability in the CuO_2 plane, $q_{CO}^{CuO_2}(x)$, levels off; concentration of 3D-AFM suppressor holes \tilde{p} ; and Sr doping x^* at the closing of the pseudogap at $T = 0$. The charge-order incommensurability in *each* LaO layer is denoted as q_{CO}^{LaO} .

Compound	\hat{x}	\tilde{p}	x^*	$q_{CO}^{CuO_2}(\hat{x})$	$q_{CO}^{CuO_2}(x^*)$	$2q_{CO}^{LaO}(x^*)$
$La_{2-x}Sr_xCuO_4$	0.125	0.015	0.18	0.235	0.235	0.235
$La_{1.6-x}Nd_{0.4}Sr_xCuO_4$	0.16	0.019	0.23	0.266	0.266	0.266

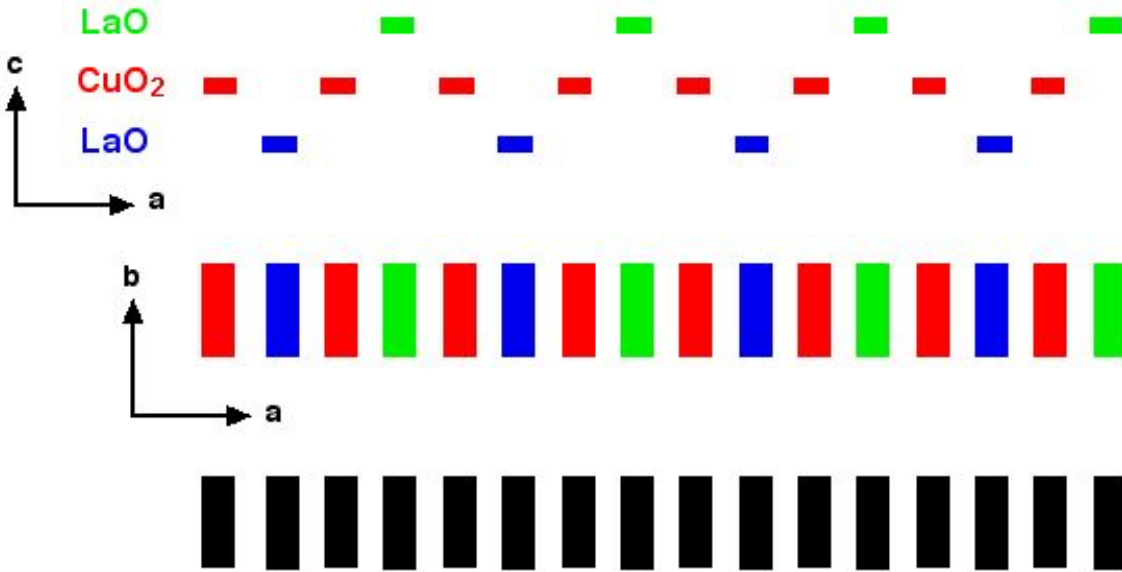


FIG. 2. Cartoon illustrating charge-order stripes in the CuO_2 plane (red), upper LaO layer (\overline{LaO} , green), and lower LaO layer (LaO , blue) in side view (top part) and down view (center and bottom part). At doping x^* , shown here, *each* LaO layer has an incommensurability $q_{CO}^{LaO}(x^*) = \frac{1}{2}q_{CO}^{CuO_2}(x^*)$. When their stripes are staggered and combined, both bracketing LaO layers *together* have the same incommensurability as the bracketed CuO_2 plane, $q_{CO}^{\overline{LaO}+LaO}(x^*) = q_{CO}^{CuO_2}(x^*)$. The stripes of the combined LaO layers are staggered against those of the CuO_2 plane such that they interlace.

Solving Eq. (4) for x^* relates the Sr -doping that causes closing of the pseudogap (at $T = 0$) with the watershed doping \hat{x} and the offset concentration \tilde{p} ,

$$x^* = \frac{3\hat{x} - \tilde{p}}{2}. \quad (6)$$

II. SELECTION OF DATA

The condition of Eq. (6) for the three parameters \hat{x} , \tilde{p} and x^* is satisfied, within error bars, for the data of $La_{2-x}Sr_xCuO_4$, listed in Table I. The offset value $\tilde{p} = 0.015 \pm 0.002$ is confirmed, through Eq. (1), by many measurements of charge-order and magnetization stripes in $La_{2-x}Sr_xCuO_4$ near $x = 0.125 = 1/8$, cited in Ref. 1. Visually, it can be inferred from the accumulation of data points *slightly above* the square-root curve in Fig. 1 (drawn with constant $\tilde{p} = x_{10} = 0.02$) for $x > 0.09$ but coincident with a slightly upshifted curve in that range (not shown) when $\tilde{p} = 0.015$ is used. The value of the watershed doping in Table I, $\hat{x} = 0.125$, is obtained by Eq. (2) from a *constant* charge-order incommensurability, $q_{CO}^{CuO_2} = 0.235, x \geq \hat{x}$, being within error bars of $q_{CO}^{CuO_2} = 0.235 \pm 0.005$ r.l.u., observed with non-resonant hard X-rays, and $q_{CO}^{CuO_2} = 0.231 \pm 0.005$ r.l.u., observed with resonant inelastic soft X-ray spectroscopy.^{2,3} The doping level where the pseudogap closes (at $T = 0$), $x^* = 0.18 \pm 0.01$, has been determined with resistivity and Nernst-effect measurements.^{4,5}

Turning to the data for $La_{1.6-x}Nd_{0.4}Sr_xCuO_4$, an offset value $\tilde{p} = 0.019$ is obtained with Eq. (1) from $q_{CO}^{CuO_2} = 0.23 \pm 0.005$ r.l.u. of $La_{1.475}Nd_{0.4}Sr_{0.125}CuO_4$.⁶ Measurements of resistivity, Hall effect, Nernst effect, and thermoelectric power give $x^* = 0.23 \pm 0.01$.⁷⁻⁹ A *constant* incommensurability of magnetization stripes, $q_M^{CuO_2} = 0.139 \pm 0.02$ r.l.u. has been observed, at temperature $T = 1.5$ K and doping $x = 0.19, 0.24, 0.26$, with neutron scattering.¹⁰ If the relationship between charge order and magnetic order,

$$q_{CO}^{CuO_2}(x) = 2q_M^{CuO_2}(x), \quad (7)$$

holds, as for $La_{2-x}Ae_xCuO_4$ ($Ae = Sr, Ba$), then $q_{CO}^{CuO_2} = 0.278$, together with Eq. (2), would give a value of $\hat{x} = 0.17 \pm 0.005$. Although close, the values of \tilde{p} , x^* and \hat{x} thusly obtained do *not* satisfy the condition of Eq. (6) *within error bars*. What could be the reason?

It is known that the magnetic moment of the co-dopant, $\mathbf{m}(Nd^{3+}) \neq 0$ — as opposed to $\mathbf{m}(La^{3+}) = 0$ — couples with the magnetic moment of the host Cu^{2+} ions, $\mathbf{m}(Cu^{2+}) \neq 0$, at temperatures $T < 5$ K.^{10,11} This is the reason why magnetization stripes are observable in $La_{1.6-x}Nd_{0.4}Sr_xCuO_4$ at such high doping, in contrast to $La_{2-x}Ae_xCuO_4$. The $\mathbf{m}(Nd^{3+})$ moments may also couple with the magnetic moments of the lattice-defect O atoms that give rise to the magnetization stripes, $\mathbf{m}(O) \neq 0$, such that the relation of Eq. (7) is slightly violated in $La_{1.6-x}Nd_{0.4}Sr_xCuO_4$. If we instead assume that Eq. (6) is valid, we

obtain $\hat{x} = (2x^* + \tilde{p})/3 = 0.16$, listed in Table I, and a charge-order incommensurability $q_{CO}^{CuO_2}(\hat{x}) = 0.266$ instead of $2q_M^{CuO_2} = 0.278$ (see Fig. 1), in slight violation of Eq. (7).

Besides $La_{2-x}Sr_xCuO_4$ and $La_{1.6-x}Nd_{0.4}Sr_xCuO_4$, treated here, there remain two more heterovalent-metal doped cuprates with high- T_c superconductivity: $La_{2-x}Ba_xCuO_4$ and $La_{1.8-x}Eu_{0.2}Sr_xCuO_4$. Because of difficulties in crystal growth, few data beyond $x = 0.125$ have been observed for $La_{2-x}Ba_xCuO_4$. With $\hat{x} = 0.14$ and $\tilde{p} = 0.015$,¹² determined by Eqs. (2, 1), a prediction of $x^* = 0.20$ can be made with Eq. (6), listed in Table II. Likewise, with $\tilde{p} = 0.015$ and $x^* = 0.23$ of $La_{1.8-x}Eu_{0.2}Sr_xCuO_4$,^{8,13} the watershed doping for that compound is predicted as $\hat{x} = 0.16$ and the constant incommensurability of charge order, $q_{CO}^{CuO_2} = 0.266$ —both in agreement with $La_{1.6-x}Nd_{0.4}Sr_xCuO_4$.

Compound	\hat{x}	$q_{CO}^{CuO_2}(\hat{x})$	\tilde{p}	x^*
$La_{2-x}Ba_xCuO_4$	0.14	0.25	0.015	0.20
$La_{1.8-x}Eu_{0.2}Sr_xCuO_4$	0.16	0.266	0.015	0.23

TABLE II: Same notations as in Table I. Predictions with Eqs. (6, 2) are marked bold.

III. SHIFT OF x^* BY Nd CO-DOPING

A question often asked is: Why is the high-doping end of the pseudogap phase different for $La_{2-x}Sr_xCuO_4$ and $La_{1.6-x}Nd_{0.4}Sr_xCuO_4$, with $x^* = 0.18$ for the former but $x^* = 0.23$ for the latter?¹⁴ If x^* is affected by the watershed doping \hat{x} , as can be inferred from Eq. (4), then the question is better rephrased as: Why is $\hat{x} = 0.125$ in $La_{2-x}Sr_xCuO_4$ but $\hat{x} = 0.16$ in $La_{1.6-x}Nd_{0.4}Sr_xCuO_4$?

It is likely that the difference is due both to different magnetic moments of co-dopant and host ions, $\mathbf{m}(Nd^{3+}) \neq \mathbf{m}(La^{3+}) = 0$, and to different ions sizes, $r(Nd^{3+}) = 1.26 \text{ \AA} < r(La^{3+}) = 1.30 \text{ \AA}$. The former gives rise to repulsive magnetic interaction between $\mathbf{m}(Nd^{3+})$ and $\mathbf{m}(O)$ moments in the $(La/Nd)O$ layers. The latter causes a slightly smaller lattice constant c_0 of the Nd -codoped compound, and consequently a slightly smaller unit-cell volume v_0 (see Table III). Conceptually, this makes it harder for doped holes to enter the $(La/Nd)O$ layers and form lattice-defect atoms, $O^{2-} + 2e^+ \rightarrow O$. The necessary higher internal pressure is achieved by Coulomb repulsion of doped holes in the CuO_2 planes at a

higher density, to wit by $\hat{x} = 0.125 \rightarrow 0.16$.

Doping \rightarrow	$x = 0$	$x = 0$	$x = 0$	$x = 0$	$x = 0.12$	$x = 0.12$	$x = 0.12$	$x = 0.12$
\downarrow Compound	a_0 (Å)	b_0 (Å)	c_0 (Å)	v_0 (Å ³)	a_0 (Å)	b_0 (Å)	c_0 (Å)	v_0 (Å ³)
$La_{2-x}Sr_xCuO_4$	5.34	5.43	13.12	380	5.33	5.36	13.18	377
$La_{1.6-x}Nd_{0.4}Sr_xCuO_4$	5.34	5.40	13.03	376	5.32	5.32	13.13	372

TABLE III: Lattice constants a_0, b_0, c_0 and unit-cell volume, $v_0 = a_0b_0c_0$, of $La_{2-x}Sr_xCuO_4$ and $La_{1.6-x}Nd_{0.4}Sr_xCuO_4$ without Sr doping, $x = 0$, and at $x = 0.12$ (Refs. 15, 16).

IV. Sr-DOPING BEYOND x^*

What happens with further Sr -doping of the lanthanum/neodymium cuprates, $x > x^*$? The constancy of $q_{CO}^{CuO_2}(x)$ for $x > x^*$, shown in Fig. 1, implies that none of the additional doped holes generate more defect O atoms in the CuO_2 plane. Neither do they generate more defect O atoms in the bracketing $(La/Sr)O$ layers — otherwise the condition of Eq. (4) would fail and the pseudogap would open again. This leaves as the most probable scenario that the additional doped holes will be *delocalized*. The assessment agrees with the notion of a Fermi-liquid phase beyond the quantum critical point, x^* , where the half-occupied $Cu d_{x^2-y^2}$ orbitals—being localized in the Mott insulator ($x < 0.02$) and in the pseudogap phase ($0.02 < x < x^*$), except when part of Fermi arcs—are now delocalized.

A transition of hole density (per Cu atom) from

$$n^+ \simeq x \quad \rightarrow \quad n^+ \simeq 1 + x \quad (8)$$

$$at \quad x < x^* < x$$

has been shown by measurements of electrical resistivity ρ , Hall coefficient R_H , and Seebeck coefficient S (thermopower) in $La_{1.6-x}Nd_{0.4}Sr_xCuO_4$.^{7,9} It can be interpreted as a massive charge delocalization. From transport measurements in $La_{1.6-x}Nd_{0.4}Sr_xCuO_4$ under pressure, a doping condition for a Lifshitz transition, $x^* \leq x^\emptyset$, was obtained.¹⁷ (A Lifshitz transition is a change of the Fermi surface between hole-like and electron-like, centered in cuprates at the M = $(\frac{1}{2}, \frac{1}{2})$ and $\Gamma = 0$ point of the Brillouin zone, respectively.) At a Lifshitz

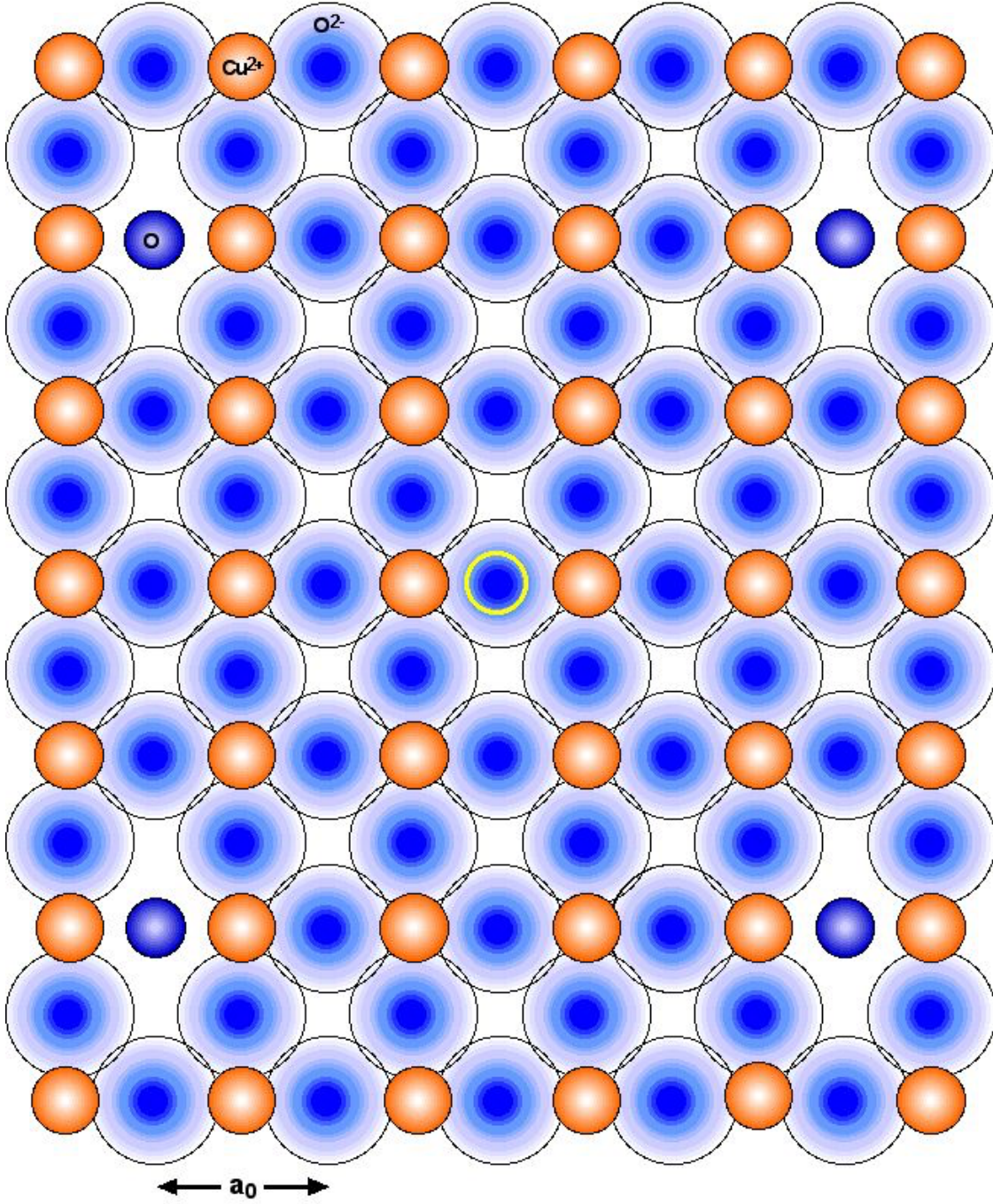


FIG. 3. Positions of host-lattice ions and lattice-defect O atoms in the CuO_2 plane, showing a unit cell of a *commensurate* O superlattice of period-4, $A_0 = 4a_0$. It is roughly comparable to the incommensurate superlattice with $A_0 = 4.25a_0$ when the pseudogap closes in $La_{2-x}Sr_xCuO_4$ or $A_0 = 3.75a_0$ for $La_{1.6-x}Nd_{0.4}Sr_xCuO_4$. A period-8 superlattice is formed by O atoms in each bracketing $(La/Sr)O$ layer — one such O atom is indicated by the yellow circle. The host lattice is shown in its *unrelaxed* position. An extended and exclusive display of all three superlattices is shown in Fig. 4.

transition the carrier density can be expected to change from holes to electrons,¹⁸

$$n^+ \simeq x \quad \rightarrow \quad n^- \simeq 1 - x \quad (9)$$

$$\text{at} \quad x < x^{\check{0}} < x.$$

It has been pointed out that the charge-density relation (8), if obtained from Hall coefficient R_H and magnetoresistivity ρ_{xx} , holds only in the high-magnetic-field limit.¹⁸ This may explain possible discrepancies between relations (8) and (9). Another issue, not completely resolved, is the Seebeck coefficient, $S > 0$, being at odds with the electron-like Fermi surface in the highly overdoped range.^{19,20}

In conclusion, no change of charge order is observed beyond closing of the pseudogap. Instead, a significant change of the band structure can be expected, along with a massive reconstruction of the Fermi surface—details of which await clarification—and entrance to the Fermi-liquid phase.

Appendix A: APPROXIMATE TREATMENT OF PSEUDOGAP CLOSING

In view of the symmetric interlacing of O -atom superlattices in the CuO_2 plane and the bracketing $(La/Sr)O$ layers, a simplified, albeit approximate, derivation of pseudogap closing can be obtained with two approximations: (i) The circumstance that the doped-hole saturated CuO_2 plane is close to a period-4 superlattice of defect O atoms, $\hat{x} \approx x_4^{CuO_2}$ (see Fig. 3). (ii) Use of *commensurate* doping concentrations for period- n superlattices, $x_n = 2/n^2$, consistent with Eq. (1) for neglected offset, $\tilde{p} = 0$. Holes doped beyond the watershed value \hat{x} settle in the $(La/Sr)O$ layers. To fill *one* such layer with a period-8 superlattice requires additional doping by $x_8^{LaO_2} = 2/8^2 = 1/32$ (yellow or green circles in Fig. 4). To fill both requires $2x_8^{LaO_2} = 2/32 = 0.0625$. As Fig. 4 shows, the O atoms of the CuO_2 plane interlace with the projection of the O atoms of the $(La/Sr)O$ layers. The total hole doping to achieve the symmetric configuration approximately is $x^{tot} = \hat{x} + 2x_8^{LaO_2} \approx x^*$ (see Table IV).

TABLE IV: Watershed concentration \hat{x} of doped Sr , hole concentration in both $(La/Sr)O$ layers, $2x_8^{LaO_2}$, total hole concentration of the approximation, x^{tot} , and quantum critical point x^* .

Compound	\hat{x}	$2x_8^{LaO_2}$	x^{tot}	x^*
$La_{2-x}Sr_xCuO_4$	0.125	0.063	0.188	0.18
$La_{1.6-x}Nd_{0.4}Sr_xCuO_4$	0.16	0.063	0.223	0.23

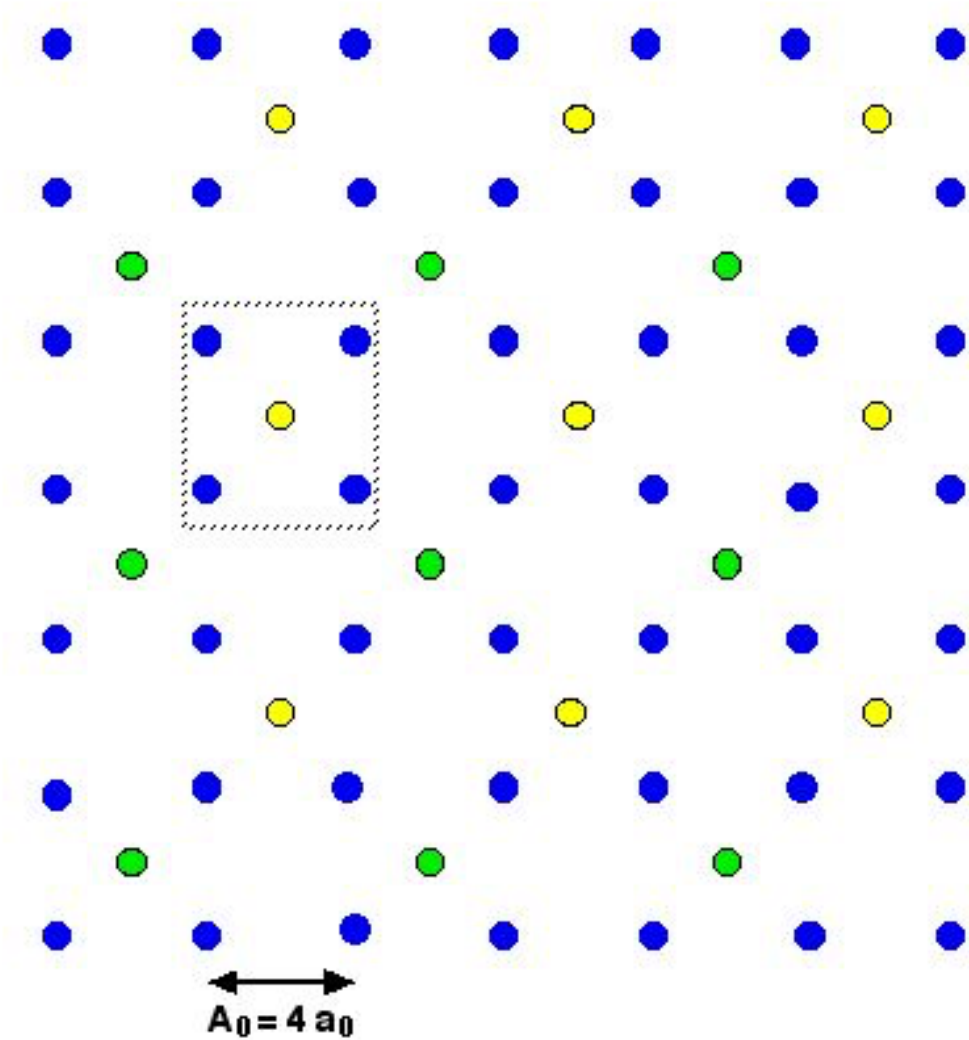


FIG. 4. Commensurate superlattices of O atoms (size exaggerated) in the CuO_2 plane (blue), upper \overline{LaO} layer (yellow), and lower \underline{LaO} layer (green). Ions of the host lattice are not shown. The framed rectangle corresponds to Fig. 3. The same symmetric pattern holds (slightly extended or contracted) for the incommensurate O superlattices when the pseudogap closes in $La_{2-x}Sr_xCuO_4$ and $La_{1.6-x}Nd_{0.4}Sr_xCuO_4$.

-
- ¹ M. Bucher, “Stripes in heterovalent-metal doped cuprates,” arXiv:2002.12116v9
- ² H. Miao, G. Fabbris, R. J. Koch, D. G. Mazzone, C. S. Nelson, R. Acevedo-Esteves, G. D. Gu, Y. Li, T. Yilimaz, K. Kaznatcheev, E. Vescovo, M. Oda, T. Kurosawa, N. Momono, T. Assefa, I. K. Robinson, E. S. Bozin, J. M. Tranquada, P. D. Johnson and M. P. M. Dean, npj Quantum Materials **6**, 31 (2021).
- ³ J. Q. Lin, H. Miao, D. G. Mazzone, G. D. Gu, A. Nag, A. C. Walters, M. García-Fernández, A. Barbour, J. Pellicciari, I. Jarrige, M. Oda, K. Kurosawa, N. Momono, K. Zhou, V. Bisogni, X. Liu, and M. P. M. Dean, Phys. Rev. Lett. **124**, 207005 (2020).
- ⁴ R. A. Cooper, Y. Wang, B. Vignolle, O. J. Lipscombe, S. M. Hayden, Y. Tanabe, T. Adachi, Y. Koike, M. Nohara, H. Takagi, C. Proust, and N. E. Hussey, Science **323**, 603 (2009).
- ⁵ O. Cyr-Choinière, R. Daou, F. Laliberté, C. Collignon, S. Badoux, D. LeBoeuf, J. Chang, B. J. Ramshaw, D. A. Bonn, W. N. Hardy, R. Liang, J.-Q. Yan, J.-G. Cheng, J.-S. Zhou, J. B. Goodenough, S. Pyon, T. Takayama, H. Takagi, N. Doiron-Leyraud, and L. Taillefer, Phys. Rev. B **97**, 064502 (2018).
- ⁶ T. J. Boyle, M. Walker, A. Ruiz, E. Schierle, Z. Zhao, F. Boschini, R. Sutarto, T. D. Boyko, W. Moore, N. Tamura, F. He, E. Weschke, A. Gozar, W. Peng, A. C. Komarek, A. Damascelli, C. Schüßler-Langeheine, A. Frano, E. H. da Silva Neto, and S. Blanco-Canosa, “Large response of charge stripes to uniaxial stress in $La_{1.475}Nd_{0.4}Sr_{0.125}CuO_4$,” arXiv:2012.09665
- ⁷ C. Collignon, S. Badoux, S. A. A. Afshar, B. Michon, F. Laliberté, O. Cyr-Choinière, J.-S. Zhou, S. Licciardello, S. Wiedmann, N. Doiron-Leyraud, and L. Taillefer, Phys. Rev. B **95**, 224517 (2017).
- ⁸ O. Cyr-Choinière, R. Daou, F. Laliberté, C. Collignon, S. Badoux, D. LeBoeuf, J. Chang, B. J. Ramshaw, D. A. Bonn, W. N. Hardy, R. Liang, J.-Q. Yan, J.-G. Cheng, J.-S. Zhou, J. B. Goodenough, S. Pyon, T. Takayama, H. Takagi, N. Doiron-Leyraud, and L. Taillefer, Phys. Rev. B **97**, 064502 (2018).
- ⁹ C. Collignon, A. Ataei, A. Gourgout, S. Badoux, M. Lizaire, A. Legros, S. Licciardello, S. Wiedmann, J.-Q. Yan, J.-S. Zhou, Q. Ma, B. D. Gaulin, N. Doiron-Leyraud, and L. Taillefer, Phys. Rev. B **103**, 155102 (2021).
- ¹⁰ Q. Ma, K. C. Rule, Z. W. Cronkwright, M. Dragomir, G. Mitchell, E. M. Smith, S. Chi, A. I.

- Kolesnikov, M. B. Stone, and B. D. Gaulin, Phys. Rev. Research **3**, 023151 (2021).
- ¹¹ J. M. Tranquada, J. D. Axe, N. Ichikawa, A. R. Moodenbaugh, Y. Nakamura, and S. Uchida, Phys. Rev. Lett. **78**, 338 (1997).
- ¹² H. Miao, R. Fumagalli, M. Rossi, J. Lorenzana, G. Seibold, F. Yakhou-Harris, K. Kummer, N. B. Brookes, G. D. Gu, L. Braicovich, G. Ghiringhelli, and M. P. M. Dean, Phys. Rev. X **9**, 031042 (2019).
- ¹³ Q. Wang, M. Horio, K. von Arx, Y. Shen, D. Mukkattukavil, Y. Sassa, O. Ivashko, C. E. Matt, S. Pyon, T. Takayama, H. Takagi, T. Kurosawa, N. Momono, S. M. Oda, T. Adachi, S. M. Haidar, Y. Koike, Y. Tseng, W. Zhang, J. Zhao, K. Kummer, M. Garcia-Fernandez, K. J. Zhou, N. B. Christensen, H. M. Rønnow, T. Schmitt and J. Chang, Phys. Rev. Lett. **124**, 187002 (2020).
- ¹⁴ A. Gourgout, A. Ataei, M.-E. Boulanger, S. Badoux, S. Thériault, D. Graf, J.-S. Zhou, S. Pyon, T. Takayama, H. Takagi, N. Doiron-Leyraud, and L. Taillefer, Phys. Rev. Research **3**, 023066 (2021).
- ¹⁵ P. G. Radaelli, D. G. Hinks, A. W. Mitchell, B. A. Hunter, J. L. Wagner, B. Dabrowski, K. G. Vandervoort, H. K. Viswanathan, and J. D. Jorgensen, Phys. Rev. **49**, 4163 (1994).
- ¹⁶ M. Dragomir, Q. Ma, J. P. Clancy, A. Ataei, P. A. Dube, S. Sharma, A. Huq, H. A. Dabkowska, L. Taillefer, and B. D. Gaulin, Phys. Rev. Materials **4**, 114801 (2020).
- ¹⁷ N. Doiron-Leyraud, Cyr-Choinière, S. Badoux, A. Ataei, C. Collignon, A. Gourgout, S. Dufour-Beauséjour, F. F. Tafti, F. Laliberté, M.-E. Boulanger, M. Matusiak, D. Graf, M. Kim, J.-S. Zhou, N. Momono, T. Kurosawa, H. Takagi, and L. Taillefer, Nat. Commun., **8**, 2044 (2017).
- ¹⁸ R.-Y. Mao, D. Wang, C. Wu, and Q.-H. Wang, “Magnetotransport in overdoped $La_{2-x}Sr_xCuO_4$: a Fermi liquid approach,” arXiv:2101.03741
- ¹⁹ A. Gourgout, G. Grissonnanche, F. Laliberté, A. Ataei, L. Chen, S. Verret, J.-S. Zhou, J. Mravlje, A. Georges, N. Doiron-Leyraud, and L. Taillefer, “Out-of-plane Seebeck coefficient of the cuprate $La_{1.6-x}Nd_{0.4}Sr_xCuO_4$ across the pseudogap critical point: particle-hole asymmetry and Fermi surface transformation,” arXiv:2106.05959
- ²⁰ H. Jin, A. Narduzzo, M. Nohara, H. Takagi, N. E. Hussey, and K. Behnia, “Positive Seebeck coefficient in highly doped $La_{2-x}Sr_xCuO_4$ ($x = 0.33$); its origin and implication,” arXiv:2101.10750